

Vertical Tunneling Graphene Heterostructure-Based Transistor for Pressure Sensing

Nayereh Ghobadi and Mahdi Pourfath, *Senior Member, IEEE*

Abstract—In this letter, a pressure sensor based on the vertical tunneling graphene field-effect transistors (VTGFETs) is proposed and theoretically analyzed. The proposed sensor consists of a graphene-hexagonal boron nitride (hBN) heterostructure. Molecular dynamic simulations are used to evaluate the strain distribution and stress-strain relation of the sensor. The device characteristics of VTGFET under pressure are investigated, by employing an atomistic tight-binding model along with the nonequilibrium Green's function formalism. The dependency of the tunneling current variation and the sensitivity on the number of hBN layers, bias voltages, and temperature are studied and appropriate parameters for optimal performance are calculated. A nonlinearity error of 3.2% within the range of 30 GPa and a sensitivity of ~ 1300 pA/A/Pa for a VTGFET with six layers of hBN are predicted.

Index Terms—Graphene, tunneling transistor, pressure sensor, quantum transport.

I. INTRODUCTION

GRAPHENE has attracted much attention due to its excellent electronic, physical, mechanical, and thermal properties. This material shows an extreme stiffness with Young's modulus of 1 TPa and a fracture strength of about 130 GPa [1] and super flexibility and stretchability up to 20% [2]. These factors render graphene as a promising base material for nano electro mechanical systems, for example for pressure sensing. The discovery of graphene in 2004 has triggered an unprecedented leap in the research on ultrathin two-dimensional crystals. Famous examples include hexagonal boron nitride (hBN) and molybdenum disulfide (MoS₂). hBN is an insulating isomorph of graphene, where boron and nitrogen atoms are organized in hexagonal rings, with a bandgap of 6 eV and a lattice mismatch with graphene of only 1.7%. hBN is comparable with graphene in terms of thermal conductivity and mechanical robustness [3]. Hybrid devices of graphene with insulating hBN have attracted the attention of scientists. Such a hetero-structure has recently been employed as a tunnel barrier in vertical graphene-based transistors [4]. The source and drain contacts of this structure are made of graphene and the tunneling barrier is composed

Manuscript received December 11, 2014; revised December 27, 2014; accepted December 31, 2014. Date of publication January 6, 2015; date of current version February 20, 2015. The review of this letter was arranged by Editor Z. Chen.

N. Ghobadi is with the Department of Electrical Engineering, University of Zanjan, Zanjan, Iran.

M. Pourfath is with the School of Electrical and Computer Engineering, University of Tehran, Tehran 14395-515, Iran, and also with the Institute for Microelectronics, Vienna University of Technology, Vienna A-1040, Austria (e-mail: pourfath@ut.ac.ir; pourfath@iue.tuwien.ac.at).

Color versions of one or more of the figures in this letter are available online at <http://ieeexplore.ieee.org>.

Digital Object Identifier 10.1109/LED.2014.2388452

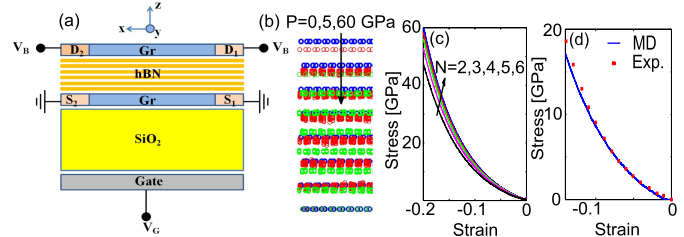


Fig. 1. (a) The sketch of the simulated VTGFET structure. All hBN layers are arranged in the Bernal (AB) stacking. A 300 nm layer of SiO₂, that corresponds to the realized structure in Ref. [4], is used as the gate oxide. The device area is 20nm². A two-electrode structure is assumed for improved electrical characteristics [5]. The drain-source bias voltage, V_B , gives rise to the tunneling current through the hBN layers. (b) The displacement of atoms in the studied structure under pressure. (c) The stress-strain relations of the VTGFET under compressive loading along the vertical direction at various numbers of hBN layers. (d) The comparison of MD simulation results with experimental data of Ref. [6].

of hBN. The operation of this device is based on the voltage tunability of the density of states in graphene and of the effective height of the tunneling barrier. In this structure, the current is due to the tunneling of carriers and exponentially increases as the thickness of the dielectric or interlayer distance of hBN layers decreases. This phenomenon makes VTGFET attractive for sensitive pressure sensing. Moreover, due to atomic thickness and lateral size of VTGFETs which can be scaled down to 10 nm [4], a footprint in the scale of nm³ can be obtained which is much smaller compared to conventional MEMS sensors. In this work, the characteristics of VTGFET-based pressure sensors are comprehensively investigated and optimization studies are performed.

II. APPROACH

The sketch of the studied VTGFET is shown in Fig. 1(a). The applied gate voltage, V_G , controls the tunneling current between source and drain by modulating the tunneling barrier height and carrier concentration. By applying pressure the sheets undergo displacement and the relative positions of atoms and interlayer distances are modified. We have utilized molecular dynamic (MD) simulations to obtain the vertical compressive strain-stress relation of VTGFETs. Based on the calculated strain values from MD simulations, the tight-binding parameters are modulated accordingly. Thereafter, the calculated interlayer distances and atomic structure of the device under pressure are used in the non-equilibrium Green's function (NEGF) formalism [7] to obtain the electrical characteristics of VTGFETs as a function of the applied pressure.

For MD simulations the large-scale atomic/molecular massively parallel simulator (LAMMPS) package has been used [8]. Periodic boundary condition is applied along the in-plane two directions. For interactions of carbon atoms in graphene sheets, the reactive empirical bond order (REBO) potential [9] is adopted. For describing the interaction between B and N atoms in boron nitride sheets, the Tersoff-like potential with the parameters proposed by Albe et al. [10] was chosen. The long-range or interlayer interactions are characterized using the Lennard-Jones 12-6 (LJ12-6) potential with the parameters from Ref. [11]. For large distances where atoms are not covalently bonded to each other and the interaction is due to van der Waals force, the LJ12-6 potential can be used. Even under strain values of about 20%, the C, B and N atoms of different layers are not close enough to interact covalently with each other and the interactions between them are still due to van der Waals force. In our simulations we assumed a unit-cell in the size of $4.26 \text{ nm} \times 4.67 \text{ nm}$. The height of the unit-cell depends on the number of hBN layers, where the thickness of each layer is assumed to be 3.35 \AA [3], [12]. The simulated cell is firstly relaxed to a minimum energy state with the conjugate gradient energy minimization. Then, in order to obtain stress-strain relation, the uniaxial strain is applied in the following way: the two graphene sheets are fixed in the vertical direction but are allowed to move in the lateral directions. Then the top graphene layer is pushed in a constant velocity along the axial direction, which results in a constant engineering strain rate of 0.05 ps^{-1} [13]. All the simulations are carried out at 300 K with the Nose-Hoover thermostat [14]. The Velocity-Verlet time stepping scheme is used with an integration time step of 0.5 fs .

The tight-binding parameters are adopted from Ref. [5]. In order to describe the modulation of the hopping parameters with the bonding length, the model proposed in Ref. [15] is employed

$$t(d) = \left(\frac{d_0}{d}\right)^2 t(d_0) \left[\frac{1}{1 + \exp[46(d/d_0 - 1)]} + \frac{(d/d_0)^{4.33} \exp[4.33(1 - d/d_0)]}{1 + \exp[-46(d/d_0 - 1)]} \right], \quad (1)$$

where d_0 and d are the undeformed and deformed bonding length/interlayer distance, respectively. This model gives more accurate results than the Harrison's model in describing the bonding length dependency of hopping parameters in layered structures [16]. For atomistic and quantum mechanical description of carrier transport in the VTGFET, the NEGF method is utilized [7]. The electrostatic potential is self-consistently evaluated [5].

III. RESULTS AND DISCUSSIONS

Fig. 1(b) shows the displacement of atoms under pressure. For a pressure range up to 60 GPa , a maximum compressive vertical strain of 20% occurs at each layer. Since graphene is a two-dimensional material, the vertical strain (ε) is defined as the ratio of the interlayer distance variation to that of the unstrained ($\varepsilon = (d_0 - d)/d_0$). The stress-strain relations of the studied structure at various numbers of hBN layers are shown

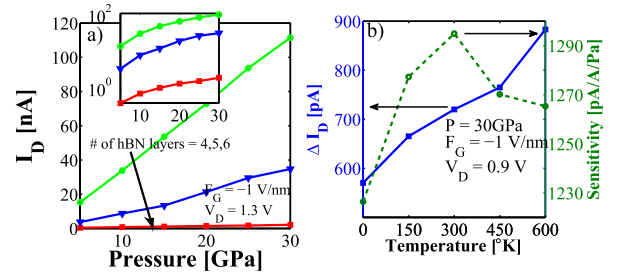


Fig. 2. (a) The drain current as function of the applied pressure (the inset shows the logarithmic scale) with 4, 5, 6 layers of hBN. (b) The variation of the tunneling current and sensitivity as functions of the temperature.

in Fig. 1(c). To validate our approach, the results of graphite are compared with experimental results [6] (Fig. 1(d)). The good agreement of our simulation results with the experimental data for graphite confirms the accuracy of our MD simulation approach. To obtain the stress-strain curve of Gr/hBN/Gr heterostructure, however, we have used the same simulation approach and the only difference is the employment of widely used Gr/hBN/Gr potential parameters [10], [11]. It should be noted that experimental values are very sensitive to the presence of stacking faults, defects, and impurities and slight deviations in theory and experiment are expected. The stress increases approximately linearly with the compressive strain at small strain values. Thereafter, it increases approximately quadratically with the strain. To obtain the same strain value, a larger stress is required as the number of layers increases which is due to stronger van der Waals interactions.

The modulation of the tunneling currents with the applied pressure are depicted in Fig. 2(a). To obtain the non-linearity error, straight lines are fitted to the curves in Fig. 2(a), using the least square method. In the range of 30 GPa , the maximum non-linearity errors for sensors with 4, 5, and 6 layers of hBN are 0.94% , 3.25% , and 3.19% , respectively. An important characteristic of a pressure sensor is its insensitivity to temperature variation. For this purpose we performed MD and NEGF simulations at various temperatures. Fig. 2(b) shows the tunneling current as a function of temperature under the pressure of 30 GPa . There are two phenomena that affect the tunneling current. Firstly, based on the Landauer formula, the tunneling current increases due to a more broadened Fermi-distribution function of carriers at higher temperatures. Secondly, at a constant pressure, sensor undergoes larger strain at higher temperature which is due to smaller elastic constant [17]. The temperature dependency of the tunneling current and the sensitivity are about $0.05\%/^{\circ}\text{C}$ and $0.01\%/^{\circ}\text{C}$ close to $T = 300\text{K}$, respectively.

An important figure of merit for a sensor is its sensitivity. The sensitivity of a pressure sensor can be defined as

$$S = \frac{\Delta I_D / I_D}{P}, \quad (2)$$

where $\Delta I_D = I_D(P = P_0) - I_D(P = 0)$ is the tunneling current variation due to pressure. The effect of the applied biases on the characteristics and sensitivity of the sensor with 6 layers of hBN is depicted in Fig. 3(a)-(c). The sensitivity peak occurs at $F_G = -1 \text{ V/nm}$ and $V_D = 0.9 \text{ V}$ which is

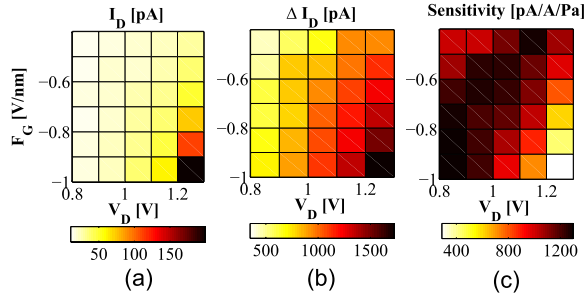


Fig. 3. (a) The drain current, (b) the drain current variations, and (c) the sensitivity of a VTGFET-based pressure sensor as functions of the applied gate and drain voltages.

TABLE I

THE SENSITIVITY AS A FUNCTION OF THE NUMBER OF hBN LAYERS

N	2	3	4	5	6	7	8
S[pA/A/Pa]	129	154	433	515	1293	1746	2827

equal to 1293 pA/A/Pa. As can be seen in Fig. 3(a) and (b), an increase in the gate and drain biases results in larger I_D and ΔI_D . Therefore both terms in the numerator and the denominator of Eq. (2) increase with an increase in bias voltages. The sensitivity peak, however, is determined by the slope of the numerator and the denominator variations. The sensitivity decreases in the region with large gate and drain voltages due to a larger tunneling current that increases the denominator of Eq. (2). On the other hand, at smaller biases, the variation of the denominator is larger than that of the numerator which results in a larger sensitivity. The temperature dependency of the sensitivity is also depicted in Fig. 2(b).

Furthermore, we investigated the effect of the number of hBN layers on the sensitivity of the sensor. The sensitivities for sensors with different hBN layers at $F_G = -1\text{V/nm}$ and $V_D = 0.9\text{V}$ are listed in Table I. The sensitivity increases with the number of hBN layers. Sensors with smaller number of hBN layers have larger I_D which increase the denominator of Eq. (2). On the other hand, at a constant pressure, sensors with larger number of hBN layers undergo smaller strains (Fig. 1(c)) which result in smaller ΔI_D and as a result the reduction of the numerator of Eq. (2). If a device with N hBN layers under the pressure P endures a strain equal to ε , the tunneling barrier thickness under the pressure P varies from $d_0 = (N + 1)3.35 \text{ \AA}$ to $d = (N + 1)(1 - \varepsilon)3.35 \text{ \AA}$. As the tunneling current has an exponential relation with the tunneling barrier, $I_D \propto \exp(-\alpha d)$ where α is a constant, the sensitivity of the device with N hBN layers can be written as $S(N) \propto I_D(P)/I_D(0) \approx \exp(\alpha(d_0 - d)) = \exp(\alpha(N + 1) \times 3.35 \times \varepsilon)$. In order to find the optimum value of N with the largest sensitivity, one must have $S(N) = S(N + 1)$. Under the same pressure P , the strain for a device with $N + 1$ hBN layers can be approximated as $\varepsilon - \Delta\varepsilon$. Using this approximation the required number of hBN layers for maximum sensitivity is $N = (\varepsilon/\Delta\varepsilon) - 2$. It can be inferred from the Fig. 1 that under the stress of 30GPa, the sensor undergoes a strain of about 0.15. $\Delta\varepsilon$ is of the order of 10^{-3} which results in N to be of the order of 100. However, this value leads to too small tunneling current for electrical detection. Thus, it is

essential to choose an appropriate value of N which results in an acceptable value of sensitivity and detectable tunneling current concurrently. As the current increases with the area of device, one can increase area to get detectable current values. As a rough estimate for sensors with nano-scale dimensions, 6-8 layers of hBN lead to simultaneous detectable tunneling current and acceptable sensitivity.

IV. CONCLUSIONS

A pressure sensor based on VTGFET is proposed. MD and atomistic NEGF simulations are employed for the analysis and optimization of such sensors. The results indicate a sensitivity of about 1300 pA/A/Pa and a temperature sensitivity of about 0.05 %/°C close to $T = 300 \text{ K}$ can be achieved for a sensor with 6 hBN layers. As the number of hBN layers increases the sensitivity increase, but the non-linearity increase and the tunneling current can become smaller than the detectable range. Excellent characteristics along with the possibility of scaling these sensors to nanometer dimensions make them excellent candidates for sensitive pressure sensing in nano electromechanical systems.

REFERENCES

- [1] C. Lee *et al.*, "Measurement of the elastic properties and intrinsic strength of monolayer graphene," *Science*, vol. 321, no. 5887, pp. 385–388, 2008.
- [2] K. S. Kim *et al.*, "Large-scale pattern growth of graphene films for stretchable transparent electrodes," *Nature*, vol. 457, no. 7230, pp. 706–710, Feb. 2009.
- [3] T. Han, Y. Luo, and C. Wang, "Effects of temperature and strain rate on the mechanical properties of hexagonal boron nitride nanosheets," *J. Phys. D, Appl. Phys.*, vol. 47, no. 2, p. 025303, 2014.
- [4] L. Britnell *et al.*, "Field-effect tunneling transistor based on vertical graphene heterostructures," *Science*, vol. 335, no. 6071, pp. 947–950, Feb. 2012.
- [5] N. Ghobadi and M. Pourfath, "A comparative study of tunneling FETs based on graphene and GNR heterostructures," *IEEE Trans. Electron Devices*, vol. 61, no. 1, pp. 186–192, Jan. 2014.
- [6] R. W. Lynch and H. G. Drickamer, "Effect of high pressure on the lattice parameters of diamond, graphite, and hexagonal boron nitride," *J. Chem. Phys.*, vol. 44, no. 1, pp. 181–184, 1966.
- [7] M. Pourfath, *The Non-Equilibrium Green's Function Method for Nanoscale Device Simulation*. Vienna, Austria: Springer-Verlag, 2014.
- [8] S. Plimpton, "Fast parallel algorithms for short-range molecular dynamics," *J. Comput. Phys.*, vol. 117, no. 1, pp. 1–19, Mar. 1995.
- [9] D. W. Brenner *et al.*, "A second-generation reactive empirical bond order (REBO) potential energy expression for hydrocarbons," *J. Phys., Condens. Matter*, vol. 14, no. 4, p. 783, 2002.
- [10] K. Albe, W. Möller, and K.-H. Heinig, "Computer simulation and boron nitride," *Radiat. Effects Defects Solids*, vol. 141, nos. 1–4, pp. 85–97, 1997.
- [11] J. H. Lee, "A study on a boron-nitride nanotube as a gigahertz oscillator," *J. Korean Phys. Soc.*, vol. 49, no. 1, pp. 172–176, 2006.
- [12] K. Min and N. R. Aluru, "Mechanical properties of graphene under shear deformation," *Appl. Phys. Lett.*, vol. 98, no. 1, p. 013113, 2011.
- [13] A. Cao and Y. Yuan, "Atomistic study on the strength of symmetric tilt grain boundaries in graphene," *Appl. Phys. Lett.*, vol. 100, no. 21, pp. 211912-1–211912-3, 2012.
- [14] W. G. Hoover, "Canonical dynamics: Equilibrium phase-space distributions," *Phys. Rev. A*, vol. 31, no. 3, pp. 1695–1697, Mar. 1985.
- [15] T. B. Boykin *et al.*, "Multiband tight-binding model for strained and bilayer graphene from DFT calculations," in *Proc. 15th Int. Workshop Comput. Electron. (IWCE)*, May 2012, pp. 1–4.
- [16] K. Khaliji *et al.*, "Tunable bandgap in bilayer armchair graphene nanoribbons: Concurrent influence of electric field and uniaxial strain," *IEEE Trans. Electron Devices*, vol. 60, no. 8, pp. 2464–2470, Aug. 2013.
- [17] W. B. Gauster and I. J. Fritz, "Pressure and temperature dependences of the elastic constants of compression-annealed pyrolytic graphite," *J. Appl. Phys.*, vol. 45, no. 8, pp. 3309–3314, Aug. 1974.